Available online at www.sciencedirect.com
SCIENCE DIRECT®
Applied Thermal Engineering 26 (2006) 1074–1086
APPLIED THERMAL ENGINEERING
www.elsevier.com/locate/apthermeng

Family design of scroll compressors with optimization

Chin-Huan Tseng [1], Yu-Choung Chang *

Department of Mechanical Engineering, National Chiao-Tung University, HsinChu 300, Taiwan

Received 5 November 2004; accepted 13 May 2005
Available online 5 January 2006

Abstract

This paper proposes a systematic design method for developing a family of scroll-type compressor (STC). Except of using the general design optimization model includes multi-variable, direct search, inequality constraints, both interactive session and discrete variable design optimization skills have also been employed in this study. A practical design case on the 5200–9800 W capacity range of the STC family using R22 refrigerant has been implemented, and to achieve a common share percentage of 80% for the major components of this STC series plus a coefficient of performance based on electrical power input (COP_{el}) of over 3.02 for each specified capacity of this family. Comparisons between calculated and measured results show that the maximum deviation of cooling capacity and COP_{el} are below 2.53% and 1.69%, respectively.

Keywords: Family design; Optimization; Scroll-type compressor; Coefficient of performance based on electrical power input (COP_{el})

1. Introduction

Simplicity, higher efficiency, quiet operation and good reliability are the special features of the scroll-type compressor (STC), a type of positive displacement compressor widely employed in residential and commercial air-conditioning, refrigeration and heat-pump applications, as well as automotive air-conditioning. Many theoretical and experimental studies have introduced and verified detailed mathematic models for STCs, including those of Morishita et al. [1,2], who derived the geometric parameters, the equations of motion and the dynamics of the scroll compressor. Ooi et al. [3], who developed the fluid flow and heat transfer used with two-dimensional numerical model in the working chamber of the STC. Several researchers [4–7] depicted an overview of the overall computer model for the STC, and Chen et al. [8,9], who presented a comprehensive model combining a detailed compression process model with a detailed overall compressor model. Based on a compilation of these prior literatures, Chang et al. [10] have implemented a computer simulation package for STC development that is used in current study.

From a technical point of view, Etemad and Nieter [11] provided a simple and easily understood optimization design approach to evaluate the effect of three relevant physical parameters on manufacturing, design limitations and energy losses for STC, and Ooi [12] presented a design optimization algorithm coupled with a mathematical model of the rolling piston compressor by employing a multi-variable, direct search, constrained optimization technique. Although these studies could provide some guides for STC optimization design algorithm and design procedure, but the detail optimum design to put in practice were not demonstrated.

One critical problem in the mass production of a variety of commercial STCs is that their key components—including fixed scroll, orbiting scroll, Oldham ring, mainframe and crankshaft—all require very high

* Corresponding author. Address: D500 ERL/ITRI, Bldg. 64, 195 ~ 6 Section 4, Chung Hsing Road, Chutung, HsinChu 310, Taiwan. Tel.: +886 3 5913367; fax: +886 3 5820250.

E-mail addresses: chtseng@cc.nctu.edu.tw (C.-H. Tseng), yuchoung@itri.org.tw (Y.-C. Chang).

[1] Tel.: +886 3 5712121x55129.

1359-4311/$ - see front matter
doi:10.1016/j.applthermaleng.2005.05.010

Nomenclature

A	clearance area (mm)
C	flow coefficient
D	diameter (mm)
F	force (N)
h	enthalpy (kJ/kg)
k	thermal conductivity (W/m °C)
L	length (m)
M	force moment (N m)
$\dot{m}$	mass flow rate (kg/h)
N	turn number of scrolls
n	polytropic index
P	power consumption (W)
p	pressure (kgf/cm^2)
r	radius (mm)
T	torque (N m)
t	thickness (mm)
V	volume rate (m^3/h)
$\dot{V}$	displacement volume (m^3/rev)
x, y	coordinates
η	efficiency
θ	rotation angle
μ	frictional coefficient
ρ	density (kg/m^3)
$\mathrm{COP_{el}}$	coefficient of performance based on electrical power input (W/W)
G_c	rigidity of cutting tool
G_w	rigidity of scroll wrap
h_e	height (mm)
p_t	pitch (mm)
Q_c	cooling capacity (W)
R_e	Reynolds number
P_r	Prandtl number
v_k	kinematic viscosity (mm^2/s)
v_r	volumetric ratio
δ_e	end side clearance between the tip and bottom of the scroll wraps (cm)
δ_a	assembly tolerance (mm)
ϕ_r	roll angle of scrolls
ω_c	rotating speed of crankshaft (rev/min)

Subscripts

B	bearing
Bd	driving bush
Bm	main journal bearing
Bl	lower journal bearing
b	base circle
d	discharge, downstream
dw	downstream
e	end surface
f	flank surface
i	inside
in	inlet
l	leakage
m	inertia force
min	minimum value
max	maximum value
motor	motor
o	outside
out	outlet
ob	orbiting scroll
or	orbiting radius
p	flate plate
r	refrigerant
s	suction
s, h	superheat
shaft	crankshaft
t	thrust
tu	tube
u	upstream
v	volumetric
w	scroll wrap
θ	tangential
1, 2	Oldham coupling surface

precision machining and skill. To help in lowering the complexity, cost and lead-time of product development, Kota et al. [13] introduced the use of commonality components in product families. In addition, Hernandez et al. [14] described a mathematical decision model for carrying out a family design evaluation for absorption chiller development that provided a guideline for the systematic design of a product family.

This paper proposes a family design procedure that combines with the optimization method [15] and the STC simulation package [10] for using in STC commercial product development to further address this problem of balancing cost, manufacturing effectiveness and product performance. Such a family design requires to meet two goals: (i) an STC with multi-specified cooling capacities have the same outside shell diameter and use common key parts or casting molds; (ii) the performance of each specified capacity of the developed STC should meet market requirements. An STC family with a range of 5200–9800 W in four models has been implemented by this research, meanwhile, the performance of each model is also verified and satisfies the required objectives.

2. Description of the design process

Fig. 1 shows the cross section and major components list of a hermetic STC used in this study. This STC's

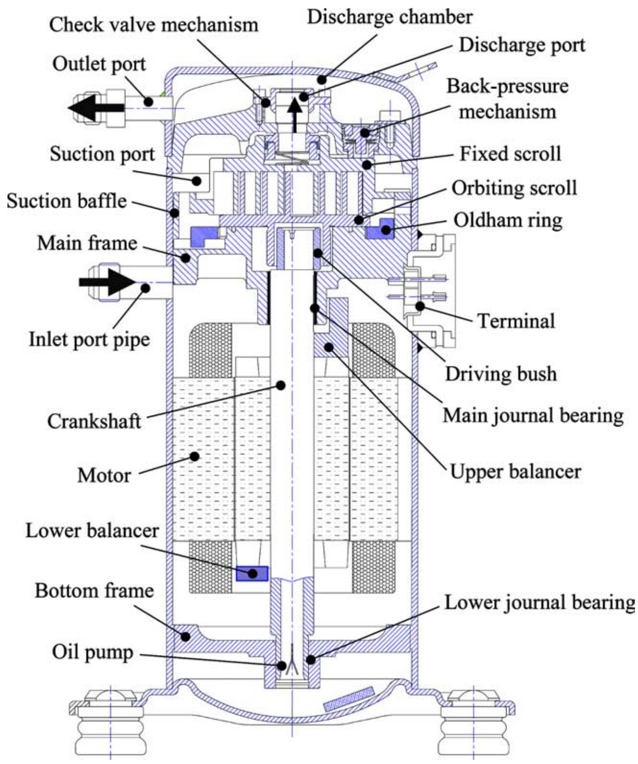

Fig. 1. The schematic and major components of a developed STC family.

structure consists of a low-pressure-shell design with a solid axial compliance mechanism applied in the fixed scroll that uses a set of backpressure mechanisms to supply solid force on the back of the fixed scroll and achieve tip-sealing behavior during STC operation [16].

In STC family design, the first decision process is to select a common outside diameter for the main shell of the STC. This selection is made based on the inside space constraints of specified air-conditioners and the motor size that can meet the torque requirements for the developed STC.

After the decision is made on the common outside diameter, the most important design process is to define the objective functions for the optimization approach. In this study, the requirement is to obtain the maximum coefficient of performance based on electrical power input ($\mathrm{COP_{el}}$) for each model of the developing STC family. Therefore, the $\mathrm{COP_{el}}$ is selected as the objective function and defined as the ratio of useful cooling capacity, $\dot{Q}_c$, to the overall power consumption of the motor, P_{motor}:

$$\mathrm{COP_{el}} = \frac{\dot{Q}_c}{P_{\mathrm{motor}}} \tag{1}$$

The next process is to define the design variables and related constraints, and then evaluate the feasible dimensions and performance for each specified STC to meet these requirements. To realize the controllable design variables and the constraint functions, the following steps are carried out.

Step 1: Define the design variables that have the most effect on the cooling capacity, $\dot{Q}_c$, and the overall power consumption of the motor, P_{motor}.

(1) The design variables of the cooling capacity, $\dot{Q}_c$: Fig. 2 shows the simplified vapor-compression refrigeration cycle that is most widely used for defining a real air-conditioning system and operating at steady conditions. When the required cooling capacity, the operating conditions and the properties of refrigerant are defined, the mass flow rate of the suction vapor inlet to the STC, $\dot{m}_s$, and the suction volume rate, $\dot{V}_s$, can be calculated thus:

$$\dot{m}_s = \frac{\dot{Q}_c}{(h_{\mathrm{in}} - h_{\mathrm{out}})} \tag{2}$$

$$\dot{V}_s = \frac{\dot{m}_s}{\rho_s} \tag{3}$$

where h_{in} and h_{out} are the enthalpies of refrigerant at evaporator inlet and outlet respectively, and ρ_s is the refrigerant density in the suction port of the STC. To obtain the properties of the refrigerant, this study uses with REFPROP 6.01 [17].

At a specified operation speed and volumetric efficiency, the displacement volume of the STC, V_d, can be estimated as follows:

$$V_d = \frac{\dot{V}_s}{\eta_v \cdot \omega_c} = \frac{\dot{m}_s}{\eta_v \cdot \omega_c \cdot \rho_s} \tag{4}$$

where volumetric efficiency, η_v, is defined as:

$$\eta_v = \frac{\dot{m}_{s,h} - \dot{m}_l}{\dot{m}_s} \tag{5}$$

The (heated) flow $\dot{m}_{s,h}$ from the suction gas inlet into the suction chamber of the scroll pump is heated by the suction import pipe and suction baffle, a process simulated in this investigation using two successive stages of turbulent flow-heated models.

In the first stage, external refrigerant flows into the compressor through a circular tube and the heat transfer coefficient conforms to the Dittus–Boelter equation [18]:

$$h_{\mathrm{tu}} = 0.023 \cdot \left(\frac{k_r}{D_i}\right) \cdot R_e^{0.8} \cdot P_r^{0.4} \tag{6}$$

In the second simulated stage, the internal refrigerant flows over a flat plate into the suction chamber for compression, and the local heat transfer coefficient conforms to the Johnson–Rubesin equation [18]:

$$h_p = 0.0296 \cdot \left(\frac{k_r}{L}\right) \cdot R_e^{0.8} \cdot P_r^{1/3} \tag{7}$$

Then, the heated suction flow rate $\dot{m}_{s,h}$ can be evaluated.

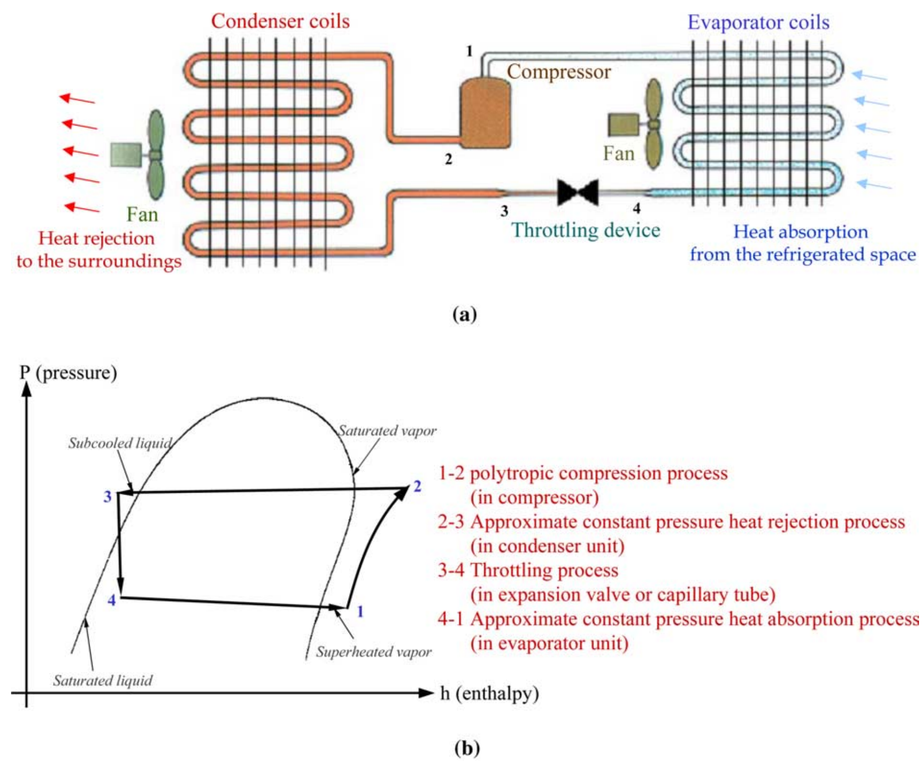

Fig. 2. The simplified refrigeration cycle for defining a real air-conditioner. (a) Schematic of vapor-compression refrigeration cycle. (b) *P–h* diagram of the cycle.

As regards the leakage flow rate $\dot{m}_l$, two types of leakage flow models have been proposed. The end side leakage is caused by a clearance area between the tip and bottom of the scroll wraps and has been given an useful model by Yanagisawa and Shimizu [19]:

$$\dot{m}_{l,e} = \frac{\pi\delta_e^3(p_i - p_o)}{6v_k \ln(r_o/r_i)} \tag{8}$$

The flank surface leakage is caused by differential pressure between the compression chambers that causes leakage to flow through a clearance area between two adjacent walls of the scroll wraps. This type of leakage flow rate can be depicted using Chu et al.'s formulation [20]:

$$\dot{m}_{l,f} = C \cdot A_f \cdot \sqrt{p_u \cdot \rho_u \cdot \frac{2n}{n-1}\left[\left(\frac{p_u}{p_{dw}}\right)^{\frac{2}{n}} - \left(\frac{p_u}{p_{dw}}\right)^{\frac{n+1}{n}}\right]} \tag{9}$$

The leakage flow rate is obtained by

$$\dot{m}_l = \dot{m}_{l,e} + \dot{m}_{l,f} \tag{10}$$

Summarizing Eqs. (2)–(10), the cooling capacity can be expressed as

$$\dot{Q}_c = \eta_v \cdot \omega_c \cdot (h_{in} - h_{out}) \cdot \rho_s \cdot V_d \tag{11}$$

Using Morishita et al.'s derivation for the STC analytical model [1], the displacement volume V_d is obtained as follows:

$$V_d = (2N - 1) \cdot \pi \cdot p_t \cdot (p_t - 2t) \cdot h_e \tag{12}$$

where N is the turn number of the scrolls and can be determined by scroll wrap roll angle:

$$\phi_r = 360^\circ \cdot \left(N + \frac{1}{4}\right) \tag{13}$$

Therefore, the cooling capacity becomes

$$\dot{Q}_c = \{\eta_v \cdot \omega_c \cdot (h_{in} - h_{out}) \cdot \rho_s\} \cdot \left\{\left[2 \cdot \left(\frac{\phi_r}{360} - \frac{1}{4}\right) - 1\right] \cdot \pi \cdot p_t \cdot (p_t - 2t) \cdot h_e\right\} \tag{14}$$

Because the refrigerant properties, operation conditions and suction paths can all be specified in the same family, the cooling capacity can be evaluated from four major design variables: ϕ_r, p_t, t and h_e. Fig. 3 shows the geometrical definitions of these four relevant design variables, which are used to define the basic dimension of the scroll set. It also illustrates how a series of cooling capacities is obtained from tuning these four design variables under the same outside diameter limitation and within certain implemental constraints.

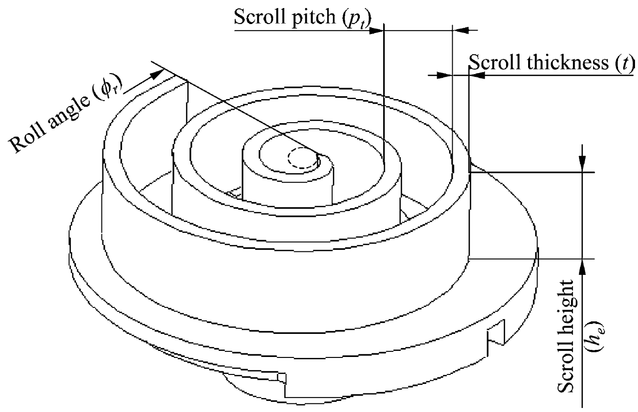

Fig. 3. Four major design variables of scroll wrap.

(2) The design variables of the overall power consumption of the motor, P_{motor}:

The overall power consumption is defined as:

$$P_{\text{motor}} = \frac{P_{\text{shaft}}}{\eta_{\text{motor}}} = \frac{T_{\text{shaft}} \cdot \omega_c}{\eta_{\text{motor}}} \tag{15}$$

The motor efficiency can be obtained by the performance test with dynamometer. The torque T_{shaft} to drive the STC is the sum of the torque that counters the tangential bearing load and the friction moment of the bearing, which is derived in detail by Morishita et al. [2]:

$$\begin{aligned} T_{\text{shaft}} &= F_{B\theta} \cdot r_{\text{or}} + \sum M_B \\ &= \{F_\theta + F_m + \mu_t F_t + (\mu_1 F_1 + \mu_2 F_2)\sin\theta_{\text{or}} \\ &\quad + (-F_1 + F_2)\cos\theta_{\text{or}}\} \cdot r_{\text{or}} + \mu_{Bd} F_{Bd} r_{Bd} \\ &\quad + \mu_{Bm} F_{Bm} r_{Bm} + \mu_{Bl} F_{Bl} r_{Bl} \end{aligned} \tag{16}$$

where $r_{\text{or}} = \frac{p_t}{2} - t$, is the orbiting radius. The first term in {} of Eq. (16) represents the gas compression force, the second term is the inertia force of acceleration (when angular velocity is constant, $F_m = 0$), and the third term is the thrust-bearing friction on the main frame. The fourth and fifth terms depict the frictional and inertia forces of the Oldham ring. The last three terms indicate the friction moments of the driving bush inside the orbiting scroll boss, main journal bearing and lower journal bearing, respectively. In Eq. (16), the frictional coefficient of each journal bearing and the Oldham coupling can all be collected by friction and wear tests [21].

If the journal bearings and the Oldham coupling used in the developed STC family are the same, it should be noted that this model makes it possible to obtain the motor efficiency and compressor speed, the several work losses and the torque T_{shaft}, and the overall power consumption P_{motor}, all can be evaluated while the design variables of p_t and t are defined.

Step 2: Set up the design constraints in order to meet the practical requirements of the scroll wrap manufacture and STC assembly.

To communicate with the engineering experts, three constraints should be considered. The rigidities of the scroll wrap and the cutting tool are the constraints for scroll wrap manufacturing, and the outside diameter limits of the scroll is the constraint for STC assembly. The correlations between design variables and constraints are defined respectively as follows:

$$G_w = \frac{h_e}{t} \tag{17}$$

$$G_c = \frac{h_e}{(p_t - t)} \tag{18}$$

$$D_{o\_max} = D_{o\_motor} - \delta_a \tag{19}$$

From involute spiral definition [22], the outmost curve coordinates that define the minimum required outside diameter D_{ob_min} of the orbiting scroll are formulated as

$$\begin{aligned} x_{ob\_o} &= r_b[\cos(\phi_r) + \phi_r \sin(\phi_r)] \\ y_{ob\_o} &= r_b[\sin(\phi_r) - \phi_r \cos(\phi_r)] \end{aligned} \tag{20}$$

where $r_b = \frac{p_t}{2\pi}$, and Eq. (20) gives the limitation for ϕ_r, p_t as

$$\begin{aligned} D_{ob\_min} &= 2 \cdot \sqrt{x_{ob\_o}^2 + y_{ob\_o}^2} = 2 \cdot r_b \sqrt{1 + (\phi_r)^2} \\ &= \frac{p_t}{\pi}\sqrt{1 + (\phi_r)^2} \leqslant D_{o\_max} \end{aligned} \tag{21}$$

$$p_t \sqrt{1 + \phi_r^2} \leqslant \pi \cdot D_{o\_max} \tag{22}$$

From Morishita et al.'s [1] derivation and Eq. (13), the roll angle of the scroll wrap has roughly obtained as

$$\phi_r \approx \frac{v_r \cdot \left(3 - \frac{\theta_d}{180^\circ}\right) + 1}{2} \cdot 360^\circ \tag{23}$$

where the built-in volumetric ratio v_r can be derived from the polytropic compression laws,

$$v_r = \left(\frac{v_s}{v_d}\right) = \left(\frac{p_d}{p_s}\right)^{\frac{1}{n}} \tag{24}$$

in which p_s and p_d are the suction and discharge pressures defined by the operation conditions depicted in Table 1 and Fig. 2. The polytropic index n can be measured by laboratory experiment [23], based on which 1.11 is selected for this study.

Eqs. (17)–(24) clearly define the constraints of ϕ_r, p_t, t and h_e for the STC family design.

Step 3: Select a proper and robust optimization algorithm to perform detailed simulation and iteration,

Table 1
Compressor operation conditions

Condensing temperature	Evaporating temperature	Degree of subcooling	Degree of superheating
54.4 °C	7.2 °C	8.3 °C	27.8 °C

and to obtain the optimum solutions for practical applications.

Summarize Eqs. (14)–(22), the objective function requirement can be defined as:

$$\text{maximize COP}_{\text{el}} = f(\phi_{\text{r}}, p_{\text{t}}, t, h_{\text{e}}) \qquad (25)$$

and subjected to the constraints:

$$\text{LowerLimits} \leqslant G_{\text{w}}, G_{\text{c}}, D_{\text{o\_max}} \leqslant \text{UpperLimits} \qquad (26)$$

As for the objective function and constraints are non-linear, the suitable optimization technique is a direct search method [12]. Meanwhile, the design variables must be monitored the progress and selected from a given set of values with practical experience. An algorithm combined with interactive session and discrete variable design optimization [15], has been employed in current study. Fig. 4 depicts the optimization process.

Interactive design optimization algorithms are based on utilizing the designer's input during the iterative process. They must be implemented into an interactive environment to report the status of the calculation results and the designer can specify what needs to be done depending on the current design conditions. In this study, an analysis module of STC simulation package

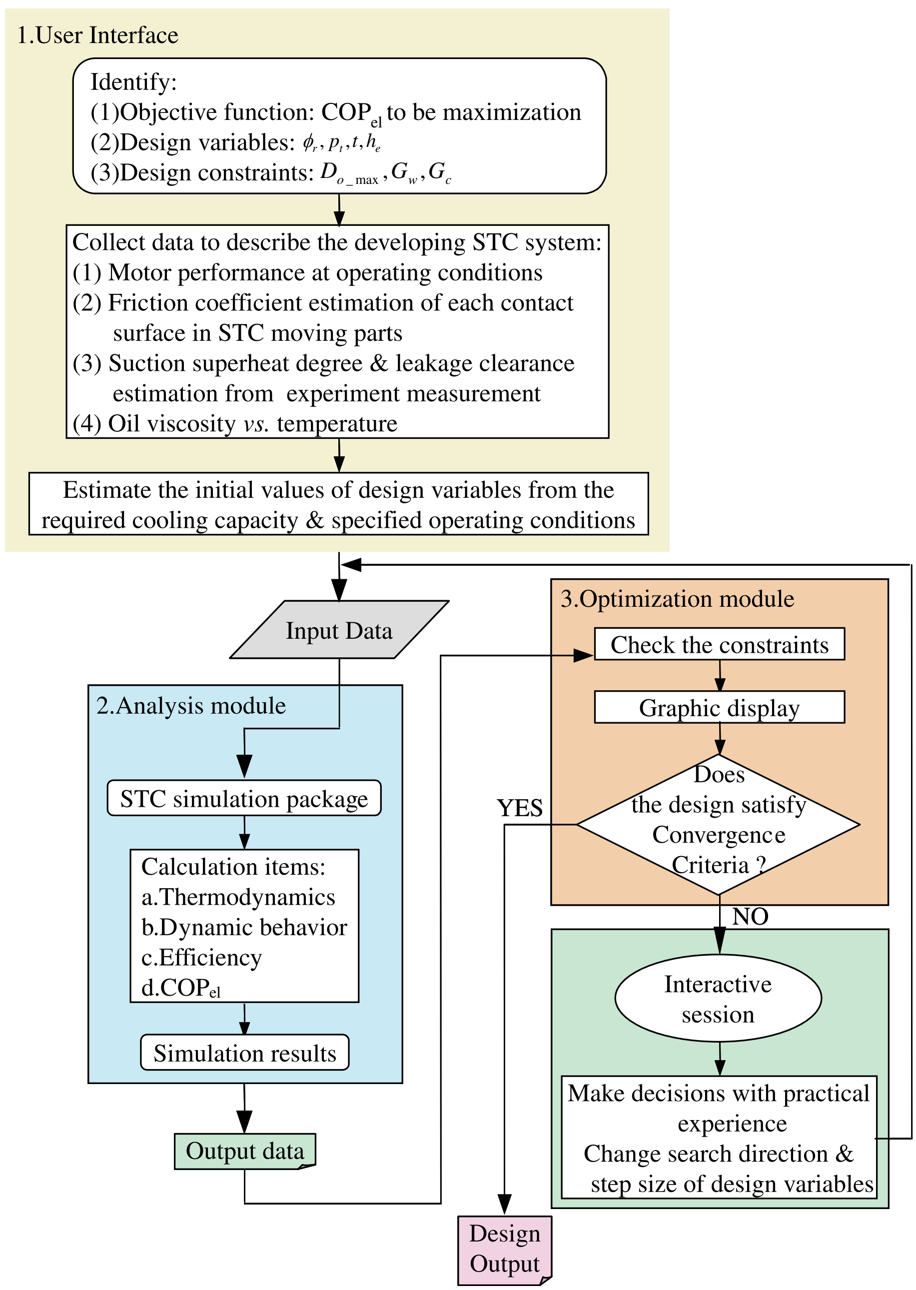

Fig. 4. The optimization process used in this study.

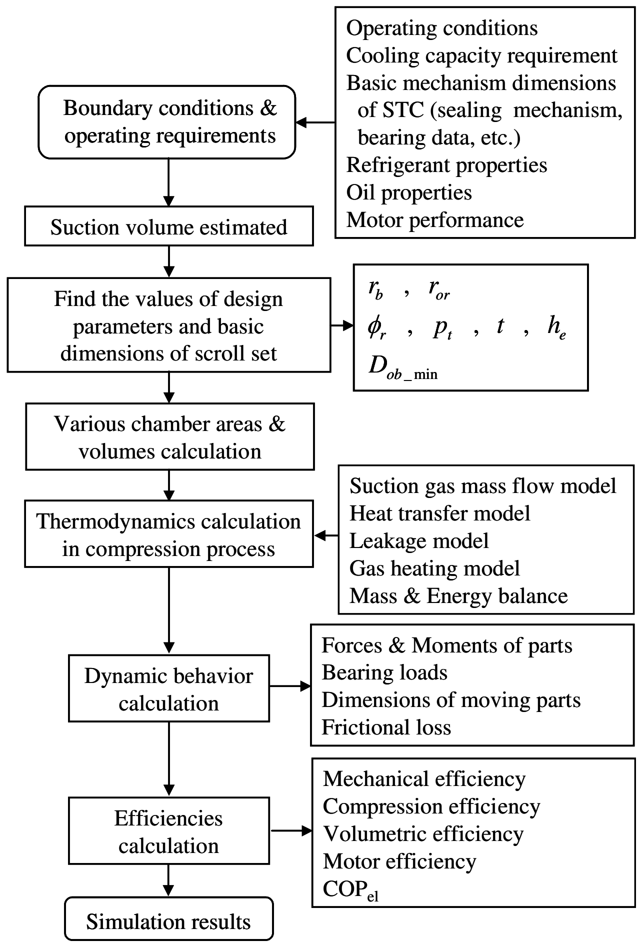

Fig. 5. The design flowchart of STC simulation package used in this study.

and graphical display to draw conclusions are to play the decision making during the interactive optimization process. Fig. 5 shows the basic simulation flowchart of the developed STC computer package.

A design variable is called discrete if its value must be selected from a given finite set of values to meet the parametric design requirements, fabrication limitations and cost effectiveness. Therefore, ϕ_r, p_t, t and h_e of four design variables all is given as discrete variables to put in practice. In the mean time, the Equal Interval Search technique [15] is used in this approach.

Using the optimization algorithm combined with a graphical solution method, the feasible region of each design variable can be identified. Finally, the optimum solutions of this family design are obtained.

3. Case study of STC family design

The required operation conditions and specifications used in the case study of STC family evaluation are given in Tables 1 and 2. The design constraints, defined in Table 3, are based on the facility limitations and capabilities of manufacturing and assembling STCs. An outside diameter of 139 mm for the motor stator is selected as the design base.

Table 2
Specifications of the STC family used in this study

Refrigerant	R-22			
Input power	220 V, single phase			
Lubricants	Mineral oil			
Shell type	Low pressure			
Compliant mechanism type	Solid axial compliant mechanism			
Motor outside diameter (mm)	139			
Specified capacity (W)	5200	6800	8100	9800
Objective of COP_{el} (W/W)	3.00	3.10	3.15	3.20

3.1. Initial design

First, the motor performance data must be collected from the motor supplier or from experiments using the dynamometer. Under the specified operational conditions (as defined in Table 1), the R22 refrigerant properties can be obtained from REFPROP 6.01 [17]. Thereafter, the theoretical pressure ratio, mass flow rate and displacement can be estimated from Eqs. (2)–(4). Depend on the suggestion of the scroll manufacturer, $t = 2.5$ mm and $\phi_r = 1050°$ are selected as initial design values. Given the limitations of the outside motor diameter and assembly tolerance, 100 mm is selected as the maximum outside diameter of the scroll set.

Table 4 shows the initial design data in this STC family development. The four design variables can be

Table 3
Design constraints

Item no.	Design constraint	Notes
1	$D_{ob\_min} \leqslant D_{o\_max} \leqslant 100$ mm	$D_{o\_motor} = 139$ mm $\delta_a \approx 40$ mm
2	$1 \leqslant G_w \leqslant 8.5$	From finite analysis of stress deflection and wrap machining capability
3	$1 \leqslant G_c \leqslant 2.5$	From cutter catalog and machining expertise

Table 4
Initial data definitions in this STC family

Required cooling capacity (W)	5200	6800	8100	9800
Displacement volume (cc)	25.4	32.3	37.4	45
Motor operating torque (N m)	3.8–4.8	4.8–5.8	5.5–6.7	6.5–8.2
Motor efficiency (%)	87	88	89	90
Cooling capacity allowance	±2%			
Motor operating speed (rpm)	3490			
Theoretical compression ratio	3.43			
Polytropic exponent	1.11			
Initial design data	$t = 2.5$ mm, $\phi_r = 1050°$			

evaluated from the equations outlined above using an iterative process.

3.2. Search direction approach

The optimization approach used in this study requires first is that a search direction for the multiple design variable variations should be identified. Figs. 6 and 7 illustrate the direction of the scroll wrap height, the sizes resulting from the different steps in the search direction approach to meet cooling capacity requirements under the constraints of D_{o_max}, G_w and G_c based on the initial design data of $t = 2.5$ mm and $\phi_r = 1050°$. These results underscore three important outcomes of using this approach:

(1) On the basis of one set of thickness t and a roll angle ϕ_r of the scroll wrap selections, Eq. (14), subjected to a change in the search direction of scroll height h_e matched with pitch p_t of the scroll wrap, can fit to each required cooling capacity requirement. The allowance has been listed in Table 4.

(2) For a specified cooling capacity requirement, increasing h_e, G_w and G_c will increase, but D_{ob_min} reduce. To meet the constraints of $D_{ob\_min} \leqslant D_{o\_max} \leqslant 100$ mm, $G_w \leqslant 8.5$, $G_c \leqslant 2.5$, the feasible region of h_e can be given. In this initial design case, the feasible region of h_e is between 16 mm and 21.3 mm. Fig. 6 has presented the approach results clearly.

(3) At specified cooling capacity, increasing h_e can improve COP_{el} as Fig. 7 shows.

3.3. Optimization process

Once the search direction of four design variables of ϕ_r, p_t, t and h_e have been tuned to meet the objective requirements for each specified cooling capacity with interactive process, the optimization approach with detail simulation and iteration is carried out.

3.3.1. First-phase evaluation

In the first-phase evaluation, the basic data variations of t are 2.5 mm to 3.3 mm with a step size of 0.05 mm ~ 0.1 mm, and ϕ_r is 1050° to 1250° with a step

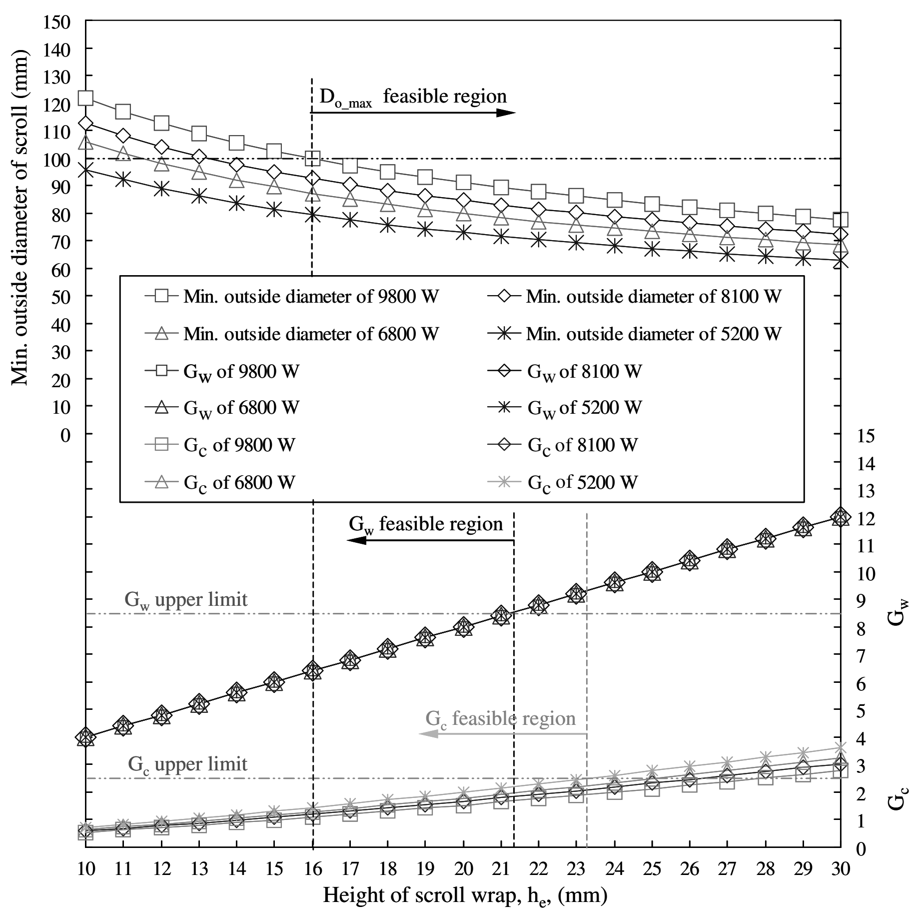

Fig. 6. Search direction approach 1 based on the initial design data.

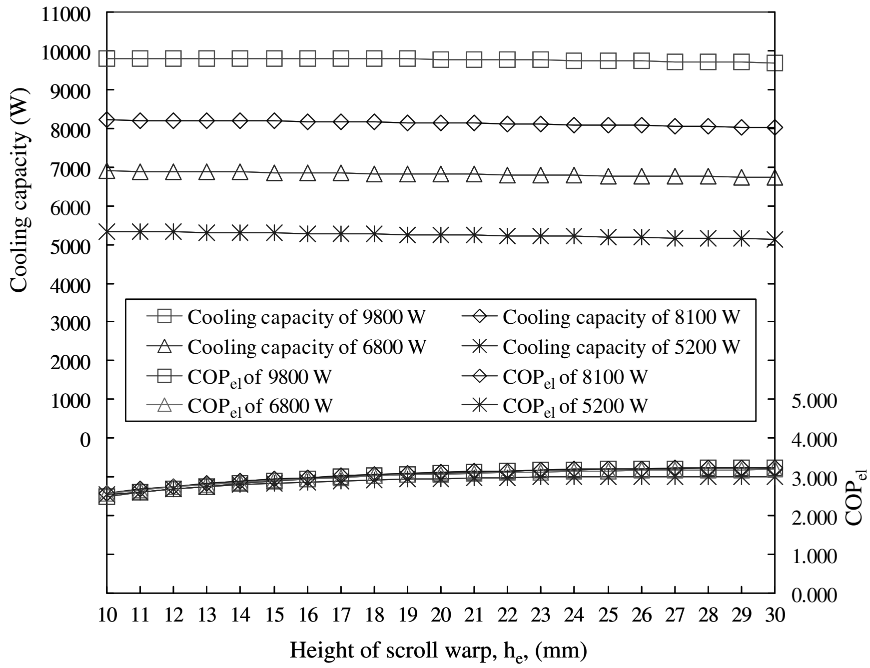

Fig. 7. Search direction approach 2 based on the initial design data.

size of 20° ∼ 50°, respectively. As shown in Table 4, by individually applying a search direction approach to each specified set of t and ϕ_r, a maximum COP$_{el}$ can be arrived at for every required cooling capacity subject to practical design limits. Fig. 8 shows the simulation data and depicts the following optimum results:

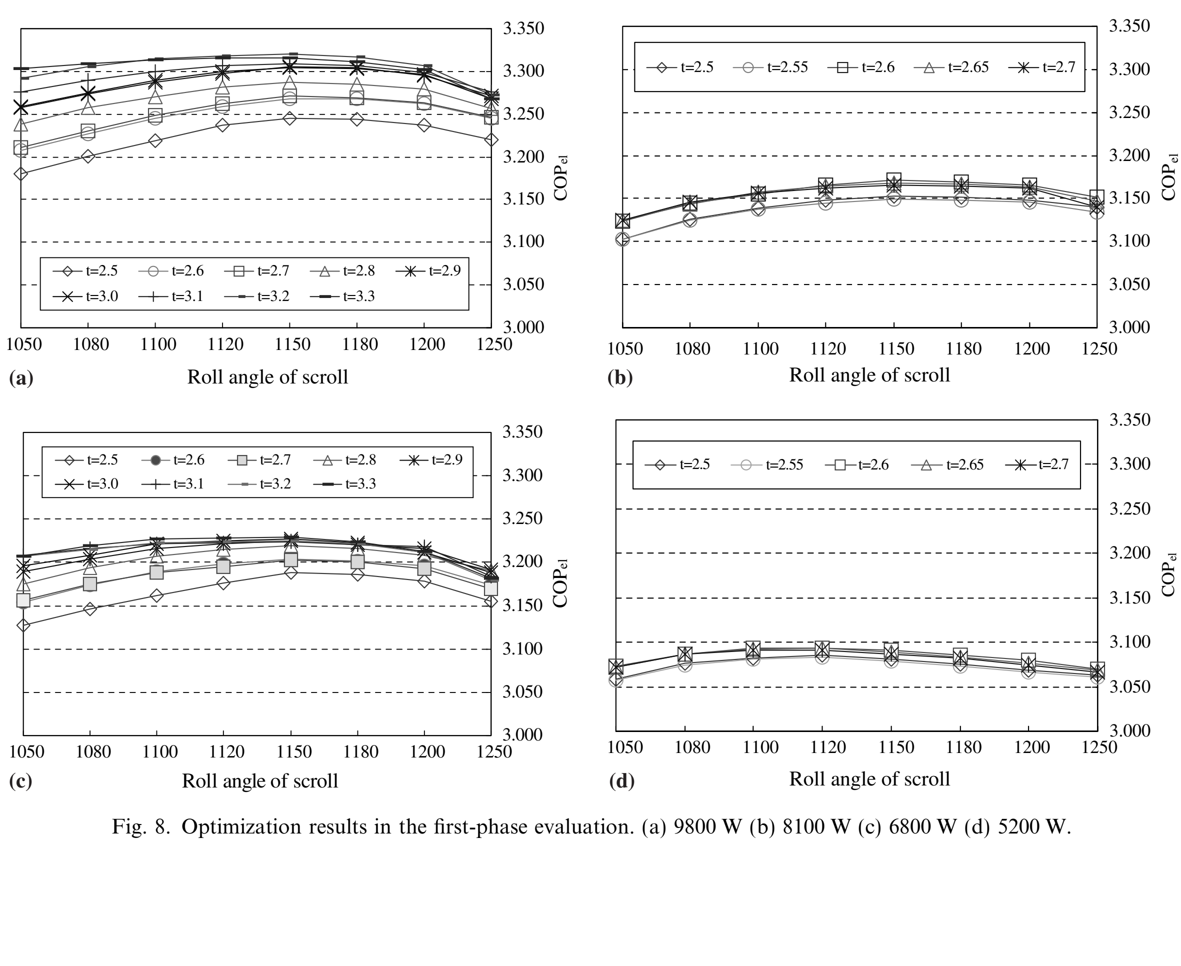

Fig. 8. Optimization results in the first-phase evaluation. (a) 9800 W (b) 8100 W (c) 6800 W (d) 5200 W.

(1) Except in the case of 5200 W, the maximum COP_{el} of each required cooling capacity in this STC family occurs at $\phi_r = 1150°$, despite various thicknesses of scroll wrap. Moreover, even though the maximum COP_{el} for 5200 W is located at $\phi_r = 1120°$, the COP_{el} deviation between 1120° and 1150° is within 0.1%.

(2) The optimum points of scroll wrap thickness are 3.2 mm, 3.3 mm, 2.6 mm and 2.6 mm for 9800 W, 8100 W, 6800 W and 5200 W, respectively. Nonetheless, for 8100 W, the COP_{el} deviation between 3.3 mm and 3.2 mm is within 0.1%. Table 5 shows the detailed design variable data for achieving the maximum COP_{el}.

(3) As a result of the above data, two thicknesses of scroll wrap are proposed to meet the objective function requirements—2.6 mm for 5200 W and 6800 W, 3.2 mm for 8100 W and 9800 W. At the same time, 1150° of roll angle is selected as the optimum value. Thereafter, only the two design variables h_e and p_t need to be tuned continuously.

3.3.2. Second-phase evaluation

As already discussed, increasing h_e can improve the COP_{el} at specified t and ϕ_r, but G_w and G_c will limit the increment of h_e. In addition, the orbiting radius of $r_{or} = \frac{p_t}{2} - t$ must also be considered because the r_{or} will influence the decision on the crankshaft dimension.

Table 5
Optimum results of first-phase evaluation

Required cooling capacity (W)	5200	6800	8100	9800
Objective of COP_{el} (W/W)	3.00	3.10	3.15	3.20
Calculated cooling capacity (W)	5224.73	6689.15	8151.13	9817.72
Calculated COP_{el} (W/W)	3.093	3.172	3.253	3.292
Thickness of scroll wrap t (mm)	2.6	2.6	3.3	3.2
Height of scroll wrap h_e (mm)	22.0	22.0	25.6	26.8
Pitch of scroll wrap p_t (mm)	11.730	12.629	13.596	14.135
Roll angle of scroll wrap ϕ_r (°)	1120	1150	1150	1150
D_{ob_min}	73.083	80.784	86.972	90.416
$G_w = h_e/t$	8.462	8.462	7.758	8.375
$G_c = h_e/(p_t - t)$	2.41	2.19	2.49	2.45

Table 6
Second-phase evaluation results

Panel a: Used with the same orbiting radius				
Calculated cooling capacity (W)	5273.15	6697.32	8181.60	9813.60
Calculated COP_{el} (W/W)	2.999	3.149	3.230	3.296
Thickness of scroll wrap t (mm)	2.6	2.6	3.2	3.2
Roll angle of scroll warp (°)	1150			
Height of scroll wrap h_e (mm)	16.524	20.952	22.605	27.2
Pitch of scroll wrap p_t (mm)	12.860	12.860	14.061	14.061
Orbiting radius $r_{or} = p_t/2 - t$	3.83			
D_{ob_min}	73.083	80.784	84.880	90.416
$G_w = h_e/t$	6.355	8.059	7.064	8.500
$G_c = h_e/(p_t - t)$	1.61	2.04	2.08	2.50
Panel b: Final optimum solutions used with two types of orbiting radius				
Calculated cooling capacity (W)	5266.15	6688.37	8181.60	9813.60
Calculated COP_{el} (W/W)	3.027	3.173	3.230	3.296
Thickness of scroll wrap t (mm)	2.6	2.6	3.2	3.2
Roll angle of scroll warp (°)	1150			
Height of scroll wrap h_e (mm)	17.427	22.100	22.605	27.200
Pitch of scroll wrap p_t (mm)	12.608	12.608	14.061	14.061
Orbiting radius $r_{or} = p_t/2 - t$	3.704		3.830	
D_{ob_min}	80.651	80.648	89.946	89.944
$G_w = h_e/t$	6.703	8.500	7.064	8.500
$G_c = h_e/(p_t - t)$	1.74	2.21	2.08	2.50

Therefore, the following two approaches are carried out in the second-phase evaluation design:

(1) The first approach uses with the same orbiting radius for the STC family. Under a maximum height of scroll wrap with G_w, G_c constraints (see Table 6(Panel a) for the solutions), the COP_{el} cannot meet the objective requirement for 5200 W.
(2) The second approach opens the restraint of the orbiting radius by drawing on the two thicknesses defined in the first-phase evaluation to propose two types of orbiting radius for this STC family. From Table 6(Panel b) shows, all result data can satisfy the COP_{el} objective requirements under specified constraints and present the final optimum solutions.

Fig. 9. One sample of the developed STC.

4. Prototyping and experimental validations

Subsequent to finding the optimum solutions for the STC family, this study implements four family prototypes. A calorimeter with a semianechonic chamber (a background noise of 40 dBA) and a sound level meter are used to measure the cooling capacity, COP_{el} and noise level of the developed STC series. Table 7 presents the specifications and measuring method of this calorimeter.

Fig. 9 shows one sample of the developed prototype, and Fig. 10 shows the comparisons of cooling capacity and COP_{el} between the experimental and calculated results. The maximum deviations for cooling capacity and COP_{el} are under 2.53% and 1.69%, respectively, suggesting that the research has successfully achieved its desired results.

Table 8 illustrates the common sharing of each major component in this STC series. In all, 58% of shared components are identical, with a total cost share of 26.85%, while 26% of shared parts are made with the same mold but have partially different dimensions, with a cost share of 62.08%. Only 16% of components, with a cost share of 11.07%, are wholly different for each specified STC in this family.

Table 7
The specifications of calorimeter used for measuring STC performance

Items	Specifications	
General description of system	According to ISO 917, this equipment is designed for fully automatic measurements	
Compressor loop refrigerant	R22	
Capacity measuring range	1500–12000 W	
Measuring method and required accuracy	(1) The equipment is employed for the secondary refrigerant system and liquid flow meter system (2) The value of the estimated error for the cooling capacity from the secondary refrigerant system calculated should be lower than liquid flow meter system (3) The deviation of cooling capacity and COP_{el} measuring results between the secondary refrigerant and liquid flow meter system should be within ±4% (4) The accuracy of refrigerant flow-measuring instruments should be within ±1% (5) The accuracy of speed-measuring instruments should be within ±0.75% (6) Repeatability ⩽ 1%	
The background noise of compressor chamber	⩽ 40 dBA when fan is closed	
Control items	**Range**	**Stability**
Compressor discharge pressure	10–30 kg/cm^2	±0.1 kg/cm^2
Compressor suction pressure	1.67–9.28 kg/cm^2	±0.15 kg/cm^2
Compressor suction temperature	−25 to 50 °C	±0.5 °C

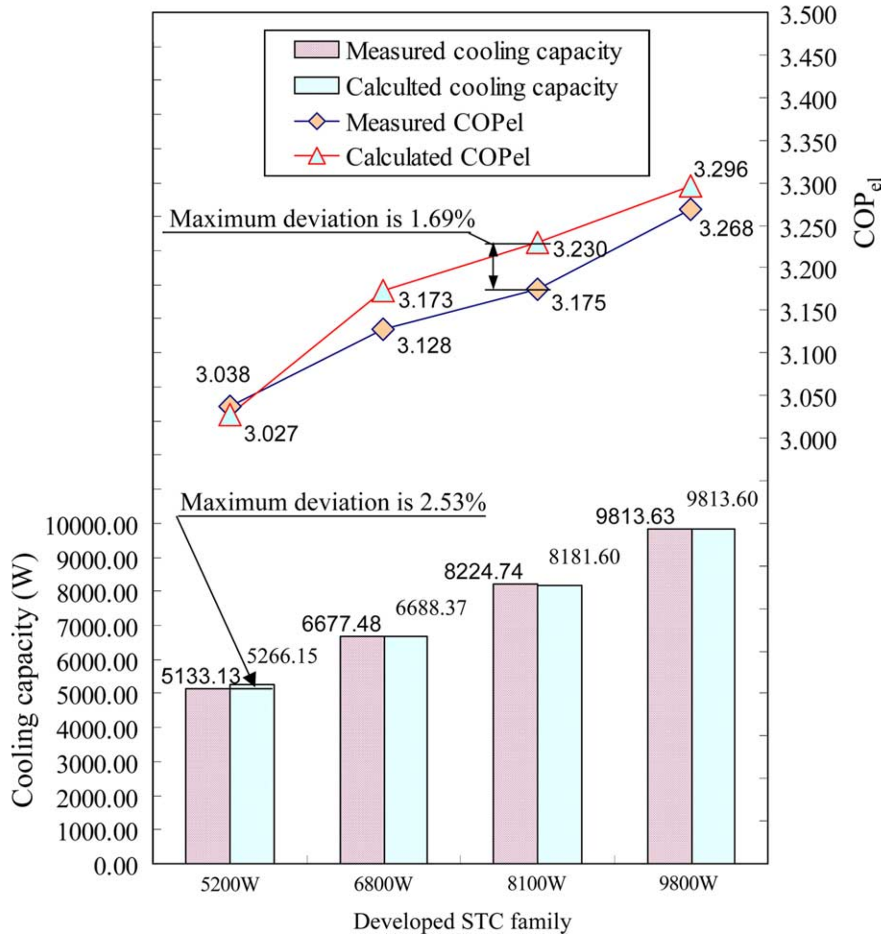

Fig. 10. Comparisons between measured and calculated results of the developed STC family.

Table 8
Common sharing status of each major component of this STC family

Component items	Common sharer	Cost share (%)	Notes
Top cover include outlet port	ˇ	3.74	One type for this series of compressor
Check valve mechanism	ˇ	1.50	One type for this series of compressor
Back pressure Mechanism	Δ	5.24	One type of casting mold but different hole diameter for different back pressure required
Fixed scroll	Δ	20.19	Two types of scroll wrap but used with same outside diameter
Orbiting scroll	Δ	19.45	Two types of scroll wrap but used with same outside diameter
Oldham ring	ˇ	1.50	One type for this series of compressor
Main frame	ˇ	11.97	One type for this series of compressor
Driving bushing	ˇ	0.15	One type for this series of compressor
Main journal bearing	ˇ	0.22	One type for this series of compressor
Upper balancer	X	0.30	Different type for each specified capacity
Main shell include inlet port and suction baffle	Δ	13.46	One type of pressing mold but different length with different capacity required
Crankshaft	X	10.47	Same shaft diameter with two types of orbiting radius and a different length for each specified capacity
Motor	Δ	3.74	One type of pressing mold but different stack height with different capacity
Lower balancer	X	0.30	Different type for each specified capacity
Terminal	ˇ	0.15	One type for this series of compressor
Bottom frame	ˇ	2.24	One type for this series of compressor
Lower journal bearing	ˇ	0.15	One type for this series of compressor
Oil pump	ˇ	2.24	One type for this series of compressor
Bottom cover	ˇ	2.99	One type for this series of compressor

1. "ˇ" means this series of STC family uses the same component.
2. "Δ" means the dimension of this component has been somewhat modified.
3. "X" means this component is different for each specified STC.

5. Conclusion

This study has demonstrated a systematic and practical process for optimization of STC family design that allows the COP_{el} for each specified capacity to meet the objective requirements of commercialization. Six important aspects of this research are summarized below:

(1) The study implemented a practical optimization algorithm combined with interactive session and discrete variables techniques, meanwhile, a developed STC simulation package and graphical display method are to play the decision making during the interactive optimization process.
(2) This investigation selected as its design variables the four geometrical factors of scroll wrap—ϕ_r, p_t, t and h_e—that can define the major dimensions of the developed STC family.
(3) Based on manufacturing and assembling expertise input, and after the COP_{el} was defined as the objective function, one case study of an STC family was developed. The calculated COP_{el} for each specified capacity of this STC family are 3.027, 3.173, 3.230, 3.296 for 5200 W, 6800 W, 8100 W, 9800 W, respectively.
(4) All STC models developed for this study met the target requirements and performance objectives. Comparisons between measured and calculated results show that the maximum deviation of cooling capacity and the COP_{el} deviation are below 2.53% and 1.69%, respectively.
(5) Two sets of scroll wrap thickness are designated, 2.6 mm for 5200 W and 6800 W, and 3.2 mm for 8100 W and 9800 W, but the dimension of the outside diameter for each specified STC in this family is identical.
(6) A common share percentage of over 80% is achieved for major components in this family design, and only 16% of components are wholly different for each specified STC.

Acknowledgement

The authors would like to express gratitude for financial support from the Energy R&D foundation funding provided by the Energy Commission of the Ministry of Economic Affairs in Taiwan.

References

[1] E. Morishita, M. Sugihara, T. Inaba, T. Nakamura, W. Works, Scroll compressor analytical model, in: Purdue International Compressor Engineering Conference Proceedings, 1984, pp. 487–495.
[2] E. Morishita, M. Sugihara, T. Nakamura, Scroll compressor dynamics (1st report, The model for the fixed radius crank), Bulletin of JSME 29 (248) (1986) 476–482.
[3] K.T. Ooi, J. Zhu, Convective heat transfer in a scroll compressor chamber: A 2-D simulation, International Journal of Thermal Science 43 (2004) 677–688.
[4] J.L. Caillat, S. Ni, M. Daniels, A computer model for scroll compressors, in: Purdue International Compressor Engineering Conference Proceedings, 1988, pp. 47–55.
[5] G.H. Lee, G.W. Kim, Performance simulation of scroll compressors, in: IMechE Conference Transactions, International Conference on Compressors and Their Systems, 2001, C591/051.
[6] C. Schein, R. Radermacher, Scroll compressor simulation model, Journal of Engineering for Gas Turbines and Power of ASME 123 (2001) 217–225.
[7] E. Winandy, C.O. Saavedra, J. Lebrun, Experimental analysis and simplified modeling of a hermetic scroll refrigeration compressor, Applied Thermal Engineering 22 (2002) 107–120.
[8] Y. Chen, N.P. Halm, E.A. Groll, J.E. Braun, Mathematical modeling of scroll compressors—Part I: compression process modeling, International Journal of Refrigeration 25 (2002) 731–750.
[9] Y. Chen, N.P. Halm, E.A. Groll, J.E. Braun, Mathematical modeling of scroll compressors—Part II: overall scroll compressor modeling, International Journal of Refrigeration 25 (2002) 751–764.
[10] Y.C. Chang, C.E. Tsai, C.H. Tseng, G.D. Tarng, L.T. Chang, Computer simulation and experimental validation of scroll compressor, in: Purdue International Compressor Engineering Conference Proceedings, 2004, p. C016.
[11] S. Etemad, J. Nieter, Design optimization of the scroll compressor, International Journal of Refrigeration 12 (1989) 146–150.
[12] K.T. Ooi, Design optimization of a rolling piston compressor for refrigerators, Applied Thermal Engineering 25 (2005) 813–829.
[13] S. Kota, K. Sethuraman, R. Miller, A metric for evaluating design commonality in product families, Journal of Mechanical Design of ASME 122 (2000) 403–410.
[14] G. Hernandez, J.K. Allen, G.W. Woodruff, T.W. Simpson, E. Bascaran, L.F. Avila, F. Salinas, Robust design of families of products with production modeling and evaluation, Journal of Mechanical Design of ASME 123 (2001) 183–190.
[15] J.S. Arora, Introduction to optimum design, Elsevier Inc., 2004.
[16] Y.C. Chang, C.H. Tseng, G.D. Tarng, L.T. Chang, Scroll compressor with solid axial sealing mechanism, in: Proceedings of the 4th International Conference on Compressor and Refrigeration, 2003, pp. 189–196.
[17] REFPROP 6.01, National Institute of Standards and Technology, Gaithersburg, MD, 1998.
[18] M.N. Ozisik, Basic heat transfer, McGraw-Hill, 1977.
[19] T. Yanagisawa, T. Shimizu, Leakage losses with a rolling piston type rotary compressor II: Leakage losses through clearances on rolling piston faces, International Journal of Refrigeration 8 (3) (1985) 152–158.
[20] I. Chu, T. Shiga, K. Ishijima, M. Sakaino, Analysis of the rolling-piston type rotary compressor, in: Purdue International Compressor Engineering Conference Proceedings, 1978, pp. 219–224.
[21] R.S. Bailey, D.G. Cutts, Journal bearing experimental evaluations and data correlation, in: Purdue International Compressor Engineering Conference Proceedings, 1996, pp. 295–302.
[22] M. Ikegawa, S. Sato, K. Tojo, A. Arai, N. Arai, Scroll compressor with self-adjusting back-pressure mechanism, ASHRAE Transactions No. 2846 Part 2A (1984) 314–326.
[23] R.L. DeBlois, R.C. Stoeffler, Instrumentation and data analysis techniques for scroll compressors, in: Purdue International Compressor Engineering Conference Proceedings, 1988, pp. 182–188.